Computer Simulation of the Dynamics of Shape Fluctuations in Uniform Star Polymers

Shu-Jun Su, Melinda S. Denny, and Jeffrey Kovac*

Department of Chemistry, University of Tennessee, Knoxville, Tennessee 37996-1600

Received March 29, 1990; Revised Manuscript Received July 16, 1990

ABSTRACT: The dynamics of uniform three- and four-arm star polymers were studied by means of Monte Carlo computer simulation. The bond fluctuation model originated by Carmesin and Kremer was extended to three dimensions and applied to the study of shape fluctuations of stars. The shape fluctuations were monitored by diagonalizing the radius of gyration tensor as a function of time and calculating the autocorrelation functions of the eigenvalues and of appropriate functions of the rotational angles extracted from the eigenvectors. These autocorrelation functions measure the two major shape relaxation processes: fluctuations of the extensions along the principal axes and rigid-body rotations. We find that the relaxation times of the fluctuations of the extensions along the principal axes ("breathing motions") obey a generalized dynamic scaling relationship. The rigid-body rotations do not relax exponentially but instead show Kohlrausch–Williams–Watts behavior.

I. Introduction

The properties of star polymers have received considerable attention in recent years, due in large part to advances in synthetic chemistry, which have facilitated the production of uniform stars with carefully controlled functionality and arm lengths. Stars with up to 56 monodisperse arms attached to a small central core have been synthesized and their properties studied experimentally.[1] This advance in experimental methodology has been accompanied by a resurgence of interest in the theory of star polymers.[2] Most of the theoretical work has focused on the conformational properties of stars as a function of both temperature and concentration. The dynamics of stars have received much less attention, however.[3,4]

In the case of star polymers it is not obvious which dynamic variables are the appropriate ones to study in order to best elucidate the motions of the molecule. Various choices have been made by previous workers. In this paper we concentrate on the shape fluctuations of stars. Although the time-averaged shape of a flexible macromolecule in free space is spherical, its instantaneous shape will instead be ellipsoidal. The study of instantaneous polymer shapes was initiated long ago by Solc and Stockmayer, who studied the radius of gyration tensor of random-flight chains. The method of analysis used in this paper was motivated by the original work of Solc and Stockmayer[5] and subsequent computer simulation studies of the shape relaxation of linear polymer by Kranbuehl, Verdier, and co-workers.[6]

A nonrigid ellipsoid has two different fundamental modes of relaxation. First, the ellipsoid can rotate without changing shape, a motion we will call a "rigid-body rotation". Second, the extensions along the principle axes can change. This latter motion is most appropriately termed a "breathing motion". In this paper we compute the radius of gyration tensor for star polymers as a function of time and analyze it using the ideas introduced above. The three-by-three radius of gyration tensor can easily be numercially diagonalized. The eigenvalues represent the extensions of the ellipsoid along its principle axes. The eigenvectors can be used to compute the angles of orientation of the principle axes of the ellipsoid with respect to a laboratory-fixed coordinate system. Appropriate autocorrelation functions of these two types of dynamical variables can then be computed and used to study the regression of shape fluctuations.

In this paper we have studied the dependence of the relaxation times of the breathing motions and the rigid-body rotation of models of isolated star polymers with excluded volume as a function of molecular weight and of the number of arms. The computer simulation model chosen is the bond fluctuation model recently developed by Carmesin and Kremer,[7] which we have implemented on a three-dimensional cubic lattice. The rigid bond lattice models[8] that we have used in the past to study the dynamics of linear polymers are not useful for stars because there are no good ways to move the branch point. The bond fluctuation model retains the advantages of lattice models while providing sufficient flexibility to allow the study of the dynamics of stars. In the three-dimensional bond fluctuation model extra care must be taken to make sure that the excluded-volume condition is rigorously maintained but the computations are still reasonably efficient.

Although a number of workers have examined the equilibrium properties of stars by means of various computer simulation techniques, there have been very few studies of the dynamics. A notable exception is the recent paper by Grest, Kremer, Milner, and Witten,[3] who studied the relaxation of self-entangled many-arm star polymers using a molecular dynamics method. Grest et al. are mainly interested in looking at the dynamics of entangled arms of stars, and so they have focused on molecules with a large number of long arms. The dynamic variables that they use to study the motions are conceptually similar to the ones used in this paper but are not identical.

In our work we have looked at only three- and four-arm stars with relatively modest molecular weights. Our main goal has been to explore the utility of the dynamic variables that we have chosen and to obtain preliminary results on the dynamics to inspire and guide future computer simulation, theoretical, and experimental studies on the dynamics of stars. Although there are no obvious experimental observables related to the shape fluctuations of stars, we feel that this work has heuristic value in that it can provide a mental picture of the motions of the molecule. Such a picture is important in both the interpretation of experiments and the construction of analytical theories.

II. Model

In this work we have adapted the two-dimensional bond fluctuation method proposed by Carmesin and Kremer. Figure 1 gives an illustration of their method. A star

0024-9297/91/2224-0917$02.50/0

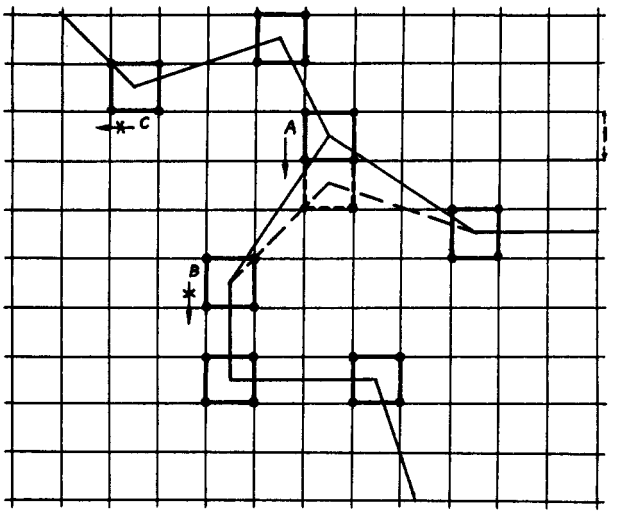

Figure 1. Illustration of the two-dimensional Carmesin–Kremer bond fluctation model.

polymer is placed on a square lattice with lattice constant 1. The bond length is required to be smaller than $(16)^{1/2}$. Each monomer occupies four lattice sites of a unit cell, and each site can be part of only one monomer (self-avoiding walk (SAW) condition). Once a monomer is chosen at random, for instance, the monomer A, it tries to randomly jump the distance of one lattice unit in one of four lattice directions. Here the monomer labeled A moved downward. This move complied with both the bond length restriction and the SAW condition and therefore was accepted. However, it would not be acceptable for the monomer B to move downward by one unit or for the monomer C to shift leftward by one unit. The former motion would be a violation of the SAW condition while the latter would lead to a bond length longer than $(16)^{1/2}$. These examples also clearly show that the set of bond vectors within the chain is not conserved.

We extended Carmesin–Kremer's two-dimensional method to a three-dimensional simple cubic lattice (SC). First, star polymers were generated on a simple cubic (SC) lattice with the arm numbers $f = 3$ and $f = 4$ and the arm lengths, N_a, of 12, 16, 20, 24, and 28 monomers. The stars were constructed on this lattice with lattice unit length 1, starting from a common center called the branch point. In three dimensions, each monomer occupies eight lattice sites of a unit cell. The SAW condition restricts each lattice site to be part of one, and only one, monomer. In this model, the bond length L, or the distance between two monomers, is not fixed. The minimum value for any L is 2, and the maximum is $(14)^{1/2}$. In between, the bond length L can have the values $(5)^{1/2}$, $(6)^{1/2}$, $(8)^{1/2}$, 3, $(10)^{1/2}$, $(12)^{1/2}$, and $(13)^{1/2}$.

A monomer randomly selected may move the distance of one lattice unit in one of six SC lattice directions subject to three conditions: the SAW condition, the bond length restriction, and no bond crossing. If the attempted move complies with all of the three criteria, it is accepted. If not, this move is abandoned and the old comformation is retained. The process is continued by the selection of a new monomer at random, and the remaining whole process is repeated. The time unit is defined as N attempted moves, where N is the total number of monomers.

Since the upper limit of the bond length $(16)^{1/2}$ will not exclude the possibility of bond crossing in the three-dimensional case as it does in the two-dimensional simulation, we further analyzed all possible cases in which an attempted move might cut through other bonds. Each attempted move would affect both the lengths of relevant bonds, i.e., the bonds between the selected monomer and its directly bonded neighbors, and their directions. Therefore, an attempted move leads to a new set of bond vectors. Depending on its relative location in a star, an attempted move made by the selected monomer might change only one bond length if the monomer is at the tail of an arm, two bond lengths if it is in the interior in an arm, or f bond lengths if it is the branch point in the chain, the center monomer. If any of bonds in the new set of bond vectors cuts through an existing bond during its formation, the bond crossing occurs and the attempted move is aborted, even though the other two conditions are met.

Unfortunately we have not found an efficient algorithm for searching for potential bond crossings. Our program proceeds by calculating the area swept out by a bond in the projected move and then systematically searching for any other bonds in the molecule that intersect that area. If such an intersection is found, the move is rejected; otherwise, it is accepted. Also, we do not allow any moves in which a monomer touches a bond. This brute force approach is rather inefficient but has not been too computationally expensive for the small molecules studied here. A more efficient algorithm is clearly needed.

Once a simulation cycle is completed, another one begins. Periodically the coordinates of all monomers in a configuration are sampled. Each run consisted of 30 000–36 000 samplings taken the cycle length of 10 times of the number of monomers ($N = N_a f + 1$) apart. To ensure an equilibrated chain, each run was begun with an initial chain configuration that was in turn the final one of the preceding run.

Since we were interested in the dynamics as well as equilibrium properties, the following quantities were calculated. The mean-square end-to-center distance is

$$\langle R^2(N_a,f)\rangle = \left\langle \frac{1}{f}\sum_{i=1}^{f}(\mathbf{r}_c - \mathbf{r}_{i,N_a})^2 \right\rangle \tag{2.1}$$

where $\mathbf{r}_{i,j}$ refers to monomer j on the arm i and site $j = N_a$ is the tail of the arm i, and $\mathbf{r}_c$ refers to the center monomer. The mean-square radius of gyration of a star polymer is

$$\langle R_G^2(N_a,f)\rangle = \left\langle \frac{1}{N_a f + 1}\sum_{i=1}^{N_a f+1}(\mathbf{r}_i - \mathbf{r}_{cm})^2 \right\rangle \tag{2.2}$$

where $\mathbf{r}_{cm}$ is the center of mass of the whole chain with

$$\mathbf{r}_{cm} = \frac{1}{N_a f + 1}\sum_{i=1}^{N_a f+1}\mathbf{r}_i \tag{2.3}$$

For the dynamic properties, we diagonalized the Solc radius of gyration tensor for the polymer.[5] Elements of this tensor are computed according to the formula

$$X_{kl} = \frac{1}{N_a f + 1}\sum_{m=1}^{N_a f+1} X_k^{(m)} X_l^{(m)} - \frac{1}{(N_a f + 1)^2}\sum_{m=1}^{N_a f+1} X_k^{(m)} \sum_{l=1}^{N_a f+1} X_l^{(l)}$$

$$l,k = 1\text{–}3 \tag{2.4}$$

where $X_k^{(m)}$ denotes the kth coordinate of the mth monomer. The ellipsoidal distribution of segments is illustrated in Figure 2.

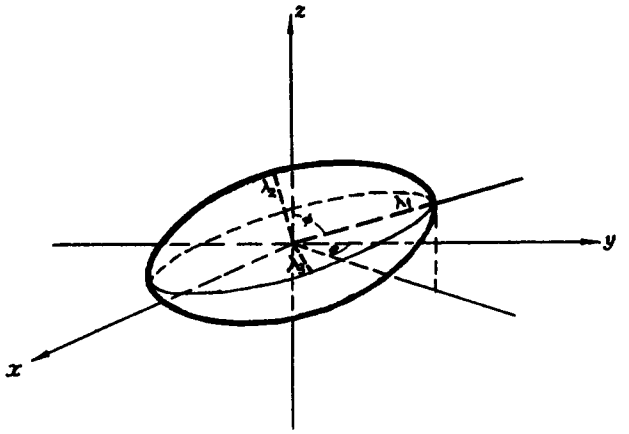

Figure 2. Ellipsoid showing principal axes and rotational angles.

The radius of gyration tensor is symmetric and can be diagonalized by a similarity transformation

$$\lambda = \mathbf{T}^{-1}\mathbf{X}\mathbf{T} \tag{2.5}$$

where $\mathbf{T}$ is the rotational matrix defined as given in eq 2.6

$$\mathbf{T} = \begin{bmatrix} \cos\phi\cos\gamma - \sin\phi\sin\gamma & \sin\phi\cos\gamma + \cos\phi\cos\theta\sin\gamma & \sin\theta\sin\gamma \\ -\cos\phi\sin\gamma - \sin\phi\cos\theta\cos\gamma & -\sin\phi\sin\gamma + \cos\phi\cos\theta\cos\gamma & \sin\theta\cos\gamma \\ \sin\phi\sin\theta & -\cos\phi\sin\theta & \cos\theta \end{bmatrix} \tag{2.6}$$

and λ is the eigenvalue matrix

$$\lambda = \begin{bmatrix} \lambda_1 & 0 & 0 \\ 0 & \lambda_2 & 0 \\ 0 & 0 & \lambda_3 \end{bmatrix} \tag{2.7}$$

The second-order spherical harmonics were then calculated as

$$Y_1 = Y_{2,0}(\theta,\phi) = -[(1/4)(5/\pi)^{1/2}(3\cos^2\theta - 1)]$$

$$Y_2 = Y_{2,+1}(\theta,\phi) = -(1/2)(15/2\pi)^{1/2}\sin\theta\cos\theta e^{+i\phi}$$

$$Y_3 = Y_{2,-1}(\theta,\phi) = (1/2)(15/2\pi)^{1/2}\sin\theta\cos\theta e^{-i\phi} \tag{2.8}$$

We constructed the autocorrelation function $C_A(t)$

$$C_A(t) = (\langle A(t)\,A(0)\rangle - \langle A\rangle^2)/(\langle A^2\rangle - \langle A\rangle^2)$$

$$A:\ R^2(N_a,f),\ R_G{}^2(N_a,f),\ \lambda_{1-3},\ Y^2{}_{1-3} \tag{2.9}$$

The ensemble averages, $\langle\cdots\rangle$, are computed as time averages over each run begun from a fully equilibrated conformation. Most of the correlation functions showed an exponential decay at long times, and so a relaxation time could be calculated by using a least-squares fit to the linear long-time region of a semilog plot of $C(t)$ vs t. For the autocorrelation function of the spherical harmonics, however, the relaxation was not a simple exponential even at long times, so the autocorrelation functions were fit to the Kohlrausch–Williams–Watts (KWW) function

$$\rho(t) = A\exp[-(t/\tau_Y)^\beta] \tag{2.10}$$

where $\rho(t)$s are the spherical harmonic autocorrelation functions. τ_Y and β are the two parameters of the KWW function: τ_Y is a relaxation time, and β is a width parameter.

Table I
Values of the Mean-Square Radius of Gyration, $\langle R_G^2\rangle$, the g Factor Defined in Equation 3.1, and the Mean-Square End-to-Center Distance for a Single Arm, $\langle R^2\rangle$

f	N_a	$\langle R_G^2\rangle$	g	$\langle R^2\rangle$	$\langle R^2(N,f)\rangle/\langle R^2(N,f=1)\rangle$[a]
3	12	71.0	0.697	176	1.11
	16	96.6	0.725	235	1.05
	20	124	0.742	303	1.03
	24	151	0.763	366	1.06
	28	178	0.758	407	1.05
4	12	56.2	0.553	127	1.14
	16	79.0	0.593	175	1.10
	20	96.5	0.578	222	1.06
	24	117	0.591	270	1.03
	28	136	0.579	324	1.05
1	36	102		159	
	48	133		224	
	60	167		294	
	72	198		367	
	84	235		387	

[a] The ratio of the end-to-center distance of an arm to the mean-square end-to-end distance of a linear polymer of the same total number of monomers as the star.

Table II
Values of the Scaling Component 2ν Defined in Equations 3.2 and 3.4 for the Molecular Size Dependence of R_G and λ_i

f	$2\nu_{R_G}$	$2\nu_1$	$2\nu_2$	$2\nu_3$
3	1.09	1.11	1.06	0.97
4	1.00	0.93	1.10	1.07
1	0.98	0.96	1.01	1.18

III. Results and Discussion

Simulations of the motions of isolated, uniform three-arm stars with arm lengths, N_a, of 12, 16, 20, 24, and 28 monomers attached to a single central monomer were performed. The four-arm stars had arm lengths, N_a, of 9, 12, 15, 18, and 21 monomers. For comparison, simulations of linear polymers with the same number of monomers were also performed. The largest molecules studied had a total of 85 monomer units. The total number of monomers is denoted by N. For the stars, $N = N_a f + 1$.

In Table I are listed the results for the equilibrium properties of the various molecules studied. We have listed the mean-square radius of gyration for linear polymers and three- and four-arm stars of the same total number of monomers, N, and computed the g factor, which is defined as

$$g = \frac{\langle R_G{}^2(N_a,f)\rangle}{\langle R_G{}^2(N,f=1)\rangle} \tag{3.1}$$

where f is the number of arms. The g factors for both types of stars are slightly smaller than those predicted by the formula of Zimm and Stockmayer.[9] We have also examined the scaling behavior of the radius of gyration by calculating the least-squares slope of a double-logarithmic plot of $\langle R_G^2\rangle$ vs $N-1$. (For consistency and for comparison with linear molecules, we have used the quantity $N-1$ as the measure of molecular size in all scaling relationships.) These slopes correspond to the exponent 2ν in the scaling relation

$$\langle R_G{}^2\rangle \sim (N-1)^{2\nu} \tag{3.2}$$

The exponents are listed in Table II. At the modest molecular sizes studied here the effects of the excluded volume do not appear strongly in the scaling behavior of

Table III
Mean Values of the Eigenvalues

f	$N-1$	$\langle\lambda_1\rangle$	$\langle\lambda_2\rangle$	$\langle\lambda_3\rangle$
3	36	43.7	16.9	5.95
	48	49.2	20.4	8.49
	60	62.7	26.4	10.5
	72	68.0	30.6	12.8
	84	77.6	33.1	15.4
4	36	32.3	15.5	6.57
	48	44.4	20.5	8.67
	60	49.9	24.4	11.3
	72	58.4	29.1	13.6
	84	64.3	32.9	15.6

R_G. This indicates that the bond fluctuation model is significantly more flexible than even the face-centered cubic lattice model that we have studied previously. The addition of a variable bond length provides an additional degree of freedom so that the chain segments can more easily avoid each other without significant expansion. It is clear that one needs to go to longer chain lengths in three dimensions to see the correct asymptotic scaling behavior in the bond fluctuation model.

We have also calculated the mean values of the eigenvalues of the radius of gyration tensor, λ_i, $i = 1$–3. These are listed in Table III for the three- and four-arm stars. Throughout this paper the eigenvalues are listed in order of decreasing size, $\lambda_1 > \lambda_2 > \lambda_3$. As expected, the four-arm stars are less aspherical than the three-arm stars. The average ratio of the three eigenvalues in the three-arm case is 5:2:1 while in the four-arm case it is 4:2:1. Both three- and four-arm stars are less aspherical than the linear chains studied here as well as those studied previously by Solc and Stockmayer[5] and by Hahn.[10] In all these cases, ratios of 15:3:1 were found for linear chains with excluded volume.

We also studied the scaling behavior of the eigenvalues, λ_i, as a function of the molecular size $N-1$. The exponents, $2\nu_i$, corresponding to the scaling relation

$$\lambda_i \sim (N-1)^{2\nu_i} \tag{3.3}$$

are listed in Table II. All these exponents are smaller than the expected value of 1.2 in the excluded-volume case. This confirms the earlier observation that the static effects of excluded volume are not evident in the scaling behavior for these molecular sizes. The exponent for the smallest eigenvalue for the linear chain does approach the expected value for the excluded-volume case. This is because the segment distribution is so compressed along this dimension that the excluded-volume effects are stronger.

Since our main interest is in the dynamics, the static scaling exponents were calculated by simple least-squares fits to the double-logarithmic plots of relaxation time vs molecular size. As pointed out by Barrett and Tremain,[2] such fits do not yield very accurate values of the exponents for the small molecular sizes studied in this paper. We have therefore only interpreted these results qualitatively. Much better Monte Carlo studies of the static properties of stars have been done by the workers cited in ref 2.

The dynamics of the stars were studied by looking at the shape fluctuations, both the breathing motions and the rigid-body rotations. The breathing motions were monitored by calculating the autocorrelation functions of the eigenvalues of the radius of gyration tensor in eqs 2.6 and 2.7. A typical autocorrelation function is shown in Figure 3. At long times the relaxation becomes a simple exponential so that a relaxation time can be extracted by fitting a least-squares line to the linear long-time region

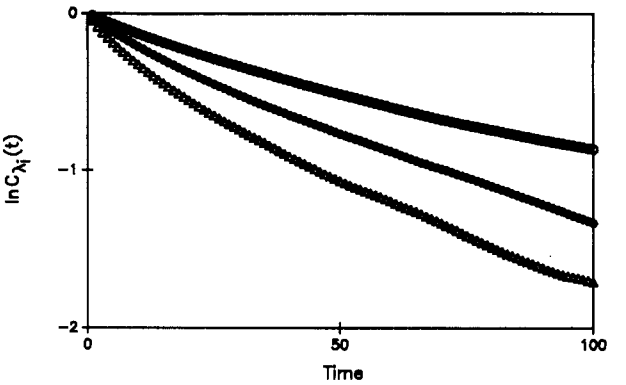

Figure 3. Plot of a typical autocorrelation function, $C_{\lambda_i}(t)$, vs time for the eigenvalue relaxation. All three eigenvalues are shown: λ_1 (○), λ_2 (●), λ_3 (△).

Table IV
Relaxation Time for the Breathing Motion

molecular size, N	no. of arms, f	arm length, N_a	relaxation time τ_{λ_1}	τ_{λ_2}	τ_{λ_3}
37	1		4400	1450	1080
	3	12	2080	1320	830
	4	9	1180	1080	709
49	1		7620	2420	1590
	3	16	4050	2190	1220
	4	12	2270	1820	1050
61	1		12700	3640	2210
	3	20	7460	3340	1530
	4	15	3940	2790	1320
73	1		18200	4770	2690
	3	24	11100	4460	2050
	4	18	6360	3730	1690
85	1		23900	6420	3220
	3	28	15500	6200	2240
	4	21	8640	5324	2050

of the semilogarithmic plot. These relaxation times are collected in Table IV.

It is interesting to compare these relaxation times to the old results of Zimm and Kilb[11] for Gaussian chains without excluded volume. Zimm and Kilb predict that the ratio of the longest relaxation time for a star of molecular size N with f branches, $\tau(N,f)$, and the longest relaxation time of a linear molecule of the same molecular size, $\tau(N,1)$, should be given by

$$\tau(N,f)/\tau(N,1) = 4/f^2 \tag{3.4}$$

We can compare our results to the prediction of Zimm and Kilb if we assume that the largest relaxation time for the breathing motions, τ_{λ_1}, is also the longest relaxation time for the molecule. For the smallest molecules studied here ($N = 37$) the Zimm–Kilb ratios are 0.47 for the three-arm star and 0.27 for the four-arm star, clearly larger than the theoretical values. For the largest molecules ($N = 85$) these ratios have increased to 0.65 and 0.36 for the two values of f. This suggests that the excluded volume increases the relaxation times of the stars more than the relaxation time of a linear molecule. This certainly makes qualitative sense.

Furthermore, we can make a few comparisons to the scaling predictions of Grest, Kremer, Milner, and Witten.[3] These authors have shown that the relaxation times for the breathing modes for stars with equal length but different numbers of arms, $\tau(N_a,f)$, should be essentially independent of f. There are a few cases among the values listed in Table I where N_a is constant or approximately constant and f varies. A comparison of these values shows that the scaling prediction seems to be qualitatively verified by our results.

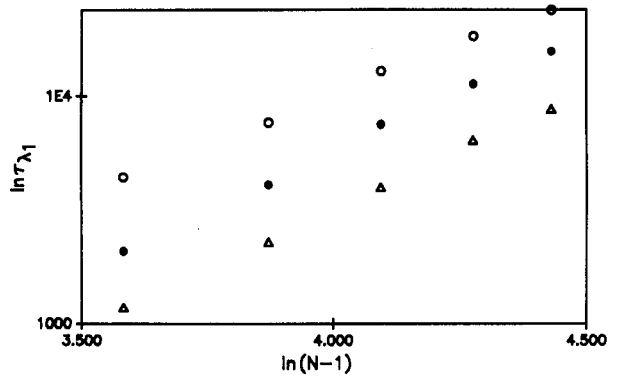

Figure 4. Scaling plot of $\ln \tau_{\lambda_1}$ vs $\ln (N-1)$ for the three molecular topologies: 1 arm (○), 3 arm (●), 4 arm (△).

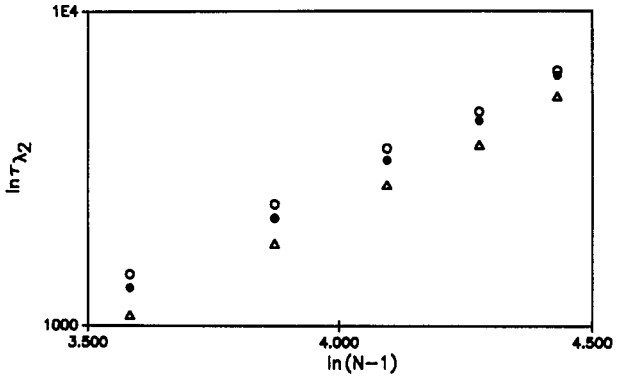

Figure 5. Scaling plot of $\ln \tau_{\lambda_2}$ vs $\ln (N-1)$ for the three molecular topologies: 1 arm (○), 3 arm (●), 4 arm (△).

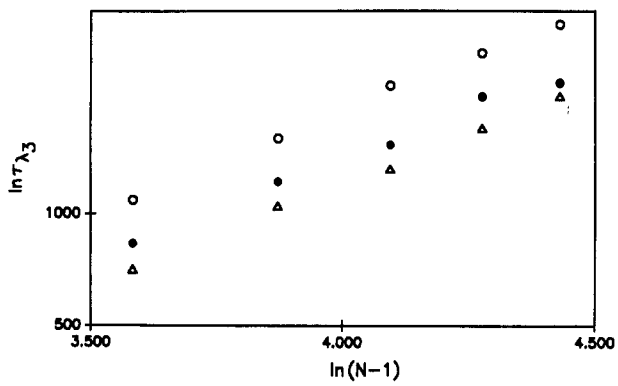

Figure 6. Scaling plot of $\ln \tau_{\lambda_3}$ vs $\ln (N-1)$ for the three molecular topologies: 1 arm (○), 3 arm (●), 4 arm (△).

Table V
Values of the Scaling Exponents, α_i, Giving the Molecular Size Reference of the Relaxation Times, τ_{λ_i}, According to the Equation $\tau_{\lambda_i} \sim (N-1)^{\alpha_i}$

f	α_1	α_2	α_3
3	1.04	0.79	0.52
4	1.04	0.81	0.54
1	0.88	0.76	0.56

Since there has been very little study of shape relaxation, the best way to further analyze these data is not obvious. Therefore, we have constructed several different scaling plots in order to try to understand the variables that primarily govern the relaxation times. In Figures 4–6 we have plotted $\ln \tau_{\lambda_i}$ vs $\ln (N-1)$ for the three different eigenvalues and the three different molecular topologies. The scaling plots are reasonably linear and yield scaling exponents, α_i, which are listed in Table V. The exponents depend strongly on which mode is being studied but are essentially independent of the number of arms. The exponents decrease as the size of the eigenvalue decreases.

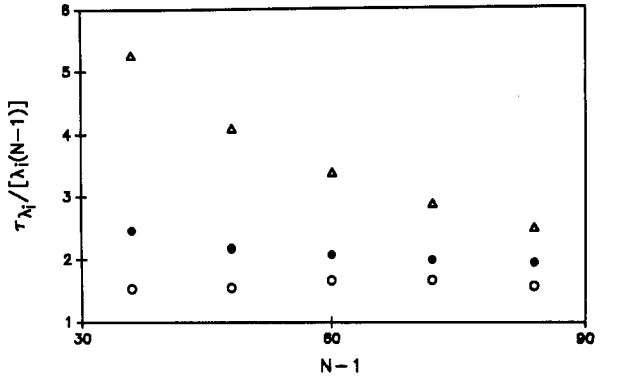

Figure 7. Plot of the ratio $\tau_{\lambda_i}/[\lambda_i(N-1)]$ vs $N-1$ for the linear molecule: λ_1 (○), λ_2 (●), λ_3 (△).

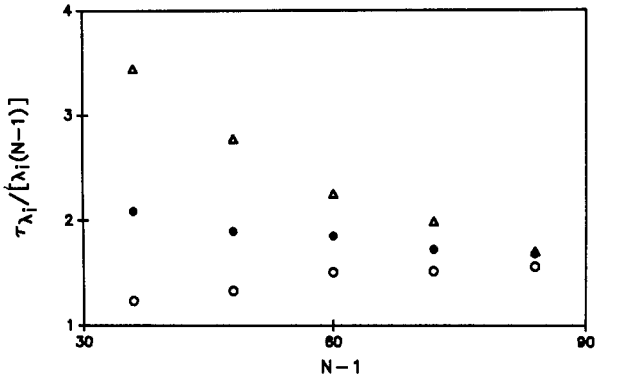

Figure 8. Plot of the ratio $\tau_{\lambda_i}/[\lambda_i(N-1)]$ vs $N-1$ for the 3-arm star: λ_1 (○), λ_2 (●), λ_3 (△).

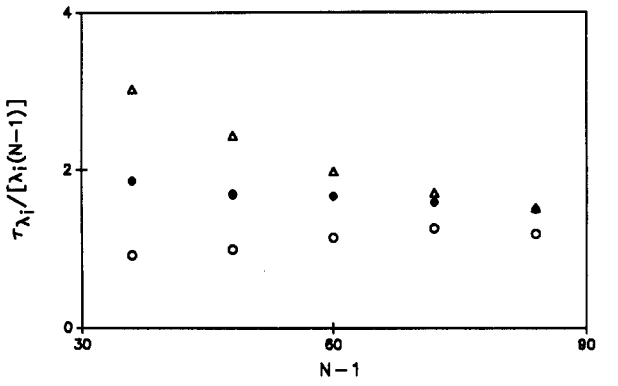

Figure 9. Plot of the ratio $\tau_{\lambda_i}/[\lambda_i(N-1)]$ vs $N-1$ for the 4-arm star: λ_1 (○), λ_2 (●), λ_3 (△).

The dynamic scaling hypothesis suggests that the relaxation times should be simply related to the molecular dimensions.[12] In the case of the eigenvalue relaxations being studied here, the appropriate scaling relation is

$$\tau_{\lambda_i} \sim \lambda_i(N-1) \tag{3.5}$$

We have investigated the validity of this hypothesis by plotting the ratio $\tau_{\lambda_i}/[\lambda_i(N-1)]$ vs $N-1$ in Figures 7–9. As can be seen from the graphs, the ratio seems to be converging to a constant that is reasonably independent of the mode being studied and of the molecular topology at large molecular sizes. We have observed this behavior before in our investigation of the dynamics of linear chains. It is interesting that the dynamic scaling hypothesis seems to be obeyed for these shape fluctuations.

The rotation of the ellipsoid was monitored by calculating the autocorrelation functions of the squares of the second-order spherical harmonics of the angles at which

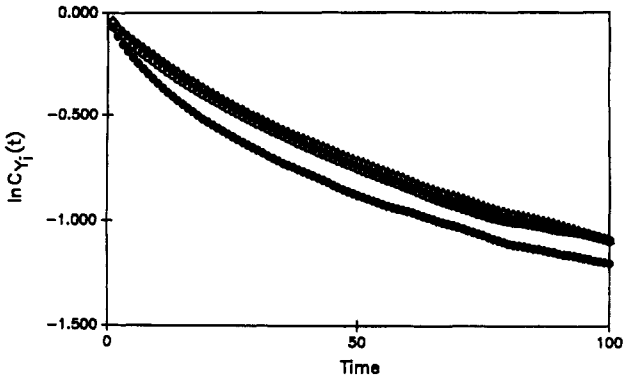

Figure 10. Plot of a typical angular relaxation autocorrelation function, $C_{Y_i}(t)$, vs time: Y_1 (○), Y_2 (●), Y_3 (△).

Table VI
Relaxation Times, τ_{Y_i} and β Values for the Body Rotation

molecular size, N	no. of arms, f	τ_{Y_i}/β		
		Y_1	Y_2	Y_3
37	1	331/0.625	399/0.524	565/0.693
	3	308/0.650	272/0.629	340/0.754
	4	209/0.676	194/0.525	220/0.722
49	1	553/0.684	546/0.555	948/0.744
	3	513/0.705	397/0.640	556/0.746
	4	391/0.652	344/0.587	365/0.754
61	1	916/0.641	900/0.592	1210/0.679
	3	771/0.672	631/0.591	802/0.725
	4	624/0.701	455/0.617	538/0.754
73	1	1310/0.628	1220/0.603	1810/0.709
	3	1190/0.667	861/0.637	1090/0.734
	4	871/0.680	584/0.598	755/0.758
85	1	1680/0.674	1450/0.615	2330/0.731
	3	1460/0.677	993/0.640	1320/0.728
	4	1130/0.642	720/0.606	995/0.760

the principal axes of the ellipsoid are oriented with respect to a fixed-coordinate system. These functions are defined in eq 2.8. Figure 10 shows a typical semilog plot of the rotational autocorrelation function. It is clear that there is no linear region even at very long times. In an effort to extract some information from these plots, we have fit them to the Kohlrausch–Williams–Watts function defined in eq 2.10. The two KWW parameters extracted from the numerical fits are listed in Table VI. Comparison of KWW relaxation times is dangerous unless the β parameters are identical. In our case the β parameter for the relaxation of each spherical harmonic is relatively independent of both molecular size and topology. Therefore, we attempted to analyze the times by constructing scaling plots of ln τ_Y vs ln $(N - 1)$, as was done for the eigenvalue relaxations. These plots, however, were far from linear even over the relatively narrow molecular size range used in our simulations. We have therefore not been able to develop any simple interpretation of the rotational behavior as measured by the spherical harmonic autocorrelation functions. It should be mentioned that similar behavior was observed by Hahn in his study of the shape fluctuations of linear simple cubic lattice model chains.[10]

Since there have been no previous studies of this rotational motion, it is difficult to interpret this result or even to decide whether it is correct. There are many processes in bulk polymers that exhibit nonexponential relaxation, and so it is tempting to suggest that the rotational dynamics of a second-order tensor field is a possible explanation for at least some of these observations. This, however, is only a speculation and deserves careful study.

Another measure of the rotation of the molecule that was suggested by Grest, Kremer, Milner, and Witten is

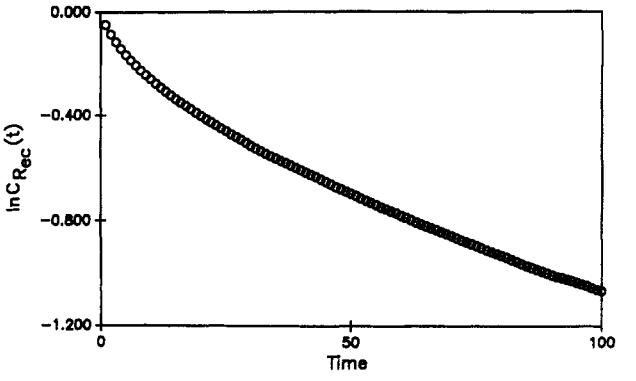

Figure 11. Plot of a typical center-to-end vector autocorrelation function, $C_{R_{ec}}(t)$, vs time.

Table VII
Relaxation Times for the End-to-Center Distance, τ_{ec}

molecular size	no. of arms	τ_{ec}
37	1	3720
	3	2180
	4	1280
49	1	6910
	3	4410
	4	2940
61	1	12500
	3	7500
	4	5260
73	1	18200
	3	12500
	4	9400
85	1	22400
	3	17600
	4	15100

Table VIII
Values of the Scaling Exponents b Defined in Equation 2.7 for the Molecular Size Dependence of R_G

f	1	3	4
b	0.92	1.08	1.26

the relaxation of the end-to-center vector of one of the arms of the star. The appropriate autocorrelation function is defined as

$$C_{ec}(t) = \langle \mathbf{R}_{ec}(t) \cdot \mathbf{R}_{ec}(0) \rangle \tag{3.6}$$

where $\mathbf{R}_{ec}$ is the center-to-end vector of one of the arms of the star. Figure 11 shows a typical autocorrelation function. This function does show an exponential decay at long times so we were able to extract a simple relaxation time, τ_{ec}, from the slope. These values are collected in Table VII. The scaling exponents, b, relating the relaxation time to the chain length as

$$\tau_{ec} \sim (N-1)^b \tag{3.7}$$

are given in Table VIII. In this case we see an increase in the exponent as the number of arms increases, suggesting that the effects of excluded volume are larger in the case of the four-arm star than in the three-arm star and linear cases. This makes sense, but it also suggests that for these small molecules with only a few arms that the center-to-end vector is not a good probe of the overall rigid-body rotation but is rather measuring the more rapid fluctuations of the arms. In the larger, more dense stars studied by Grest, Kremer, Milner, and Witten this quantity is probably more representative of the overall molecular motion because the arms have less freedom to move independently of the whole molecule.

An interesting question that can be examined by our analysis of the motion of stars is whether *the rotational*

and breathing motions occur on widely different time scales. The nonexponential behavior of the rotational relaxation makes this comparison more difficult, but some qualitative observations can be made. Comparison of the relaxation times listed in Tables IV and VI shows that the rotational motions are faster than the breathing motions. The ratio of the fastest breathing motion time to the slowest rotational time decreases as the molecular size increases. For the largest molecules the ratio is approximately 2. Since the rotations are followed by studying the square of the spherical harmonics, the times obtained are a factor of 2 smaller than those that would be measured by autocorrelation functions of the spherical harmonics themselves. This means that the slowest actual rotational relaxation times are comparable to the fastest breathing motion times for the largest molecules. It will be interesting to see whether this ratio remains constant as the molecular size increases even further or whether it decreases even further.

On the basis of the data we have obtained in this study, it seems that there is no clear time-scale separation between the rotational motions and the breathing motions. The rotations are faster, but the time scales overlap for the larger molecules. It is important to see whether this pattern continues as the molecular weight increases and to study the effects of concentration on the time scales of these two modes of motion. These are questions we plan to pursue.

IV. Conclusion

In this paper we have studied the shape fluctuations in three- and four-arm uniform star polymers using the bond fluctuation model. These fluctuations have been analyzed by diagonalizing the radius of gyration tensor and studying the decay of the autocorrelation functions of both the eigenvalues and the eigenvectors. The eigenvalues probe the breathing motions of the molecule, while the eigenvectors monitor the rotational motion.

The relaxations of the eigenvalues seem to obey a generalized dynamic scaling relationship. The faster rotational motions, however, do not decay exponentially even at very long times. They can be fit by a KWW function so a characteristic relaxation time can be extracted from the decay of the autocorrelation functions. These relaxation times do not seem to obey a simple scaling relation, however. The time scales of the two types of motions seem to be converging as the molecular size increases.

These results show that shape fluctuations can be used to study the motions of star polymers. They provide a fairly clear physical picture of the molecular motion. The question that needs to be answered is whether this method of analysis will carry over into the study of concentrated systems and provide any insight into the behavior of bulk polymers. We plan to pursue this question in forthcoming publications.

Acknowledgment is made to the U.S. Department of Energy, Office of Basic Energy Sciences, Division of Materials Sciences, for financial support of this work. We also thank the University of Tennessee Computing Center for their continuing support. M.S.D. was supported by the UTK Science Alliance as a summer undergraduate research student in 1988. J.K. gratefully recalls an ancient conversation with Robert Zwanzig, which stimulated his interest in the relaxation of second-rank tensor quantities. We also thank E. Todd Ryan, Thomas D. Hahn, and Rajiv R. Singh for useful conversations during the course of this work.

References and Notes

(1) Bauer, B. J.; Fetters, L. J.; Graessley, W. W.; Hadjichristidis, N.; Quack, G. F. *Macromolecules* **1989**, *22*, 2337.
(2) Daoud, M.; Cotton, J. P. *J. Phys. (Paris)* **1982**, *43*, 531. Birshtein, T. M.; Zhulina, E. B. *Polymer* **1984**, *25*, 1984. Birshtein, T. M.; Zhulina, E. B.; Borisov, O. V. *Polymer* **1986**, *27*, 1078. Barrett, A. J.; Tremain, D. L. *Macromolecules* **1987**, *20*, 1687. Grest, G. S.; Kremer, K.; Witten, T. A. *Macromolecules* **1987**, *20*, 1376. Batoulis, J.; Kremer, K. *Macromolecules* **1989**, *22*, 4277. Whittington, S. G.; Lipson, J. E. G.; Wilkinson, M. K.; Gaunt, D. S. *Macromolecules* **1986**, *19*, 1241. Miyake, A.; Freed, K. F. *Macromolecules* **1983**, *16*, 1228; *Macromolecules* **1984**, *17*, 678.
(3) Grest, G. S.; Kremer, K.; Milner, S. T.; Witten, T. A. *Macromolecules* **1989**, *22*, 1904.
(4) Bishop, M.; Clarke, J. H. R. *J. Chem. Phys.* **1989**, *90*, 6647.
(5) Solc, K.; Stockmayer, W. H. *J. Chem. Phys.* **1971**, *54*, 2756. Solc, K. *J. Chem. Phys.* **1971**, *55*, 335.
(6) Kranbuehl, D. E.; Verdier, P. H.; Spencer, J. M. *J. Chem. Phys.* **1973**, *59*, 3861. Kranbuehl, D. E.; Verdier, P. H. *J. Chem. Phys.* **1977**, *67*, 361.
(7) Carmesin, I., Kremer, K. *Macromolecules* **1988**, *21*, 2819.
(8) Crabb, C. C.; Hoffman, D. F., Jr.; Dial, M.; Kovac, J. *Macromolecules* 1988, *21*, 2230 and references therein.
(9) Zimm, B. H.; Stockmayer, W. H. *J. Chem. Phys.* **1949**, *17*, 1301.
(10) Hahn, T. D. M.S. Thesis, University of Tennessee, 1989.
(11) Zimm, B. H.; Kilb, R. W. *J. Polym. Sci.* **1959**, *37*, 19.
(12) de Gennes, P.-G. *Scaling Concepts in Polymer Physics*; Cornell University Press: Ithaca, NY, 1979.